Jurnal Teknologi, 46(A) Jun 2007: 53–72

THE PERFORMANCE OF SEMI-METALLIC FRICTION MATERIALS FOR PASSENGER CARS

RIA JAAFAR TALIB[1*], ANDANASTUTI MUCHTAR[2] & CHE HUSNA AZHARI[3]

Abstract. In this work, a semi-metallic friction material for passenger cars was evaluated for mechanical wear by pressing the material against a rotating pearlitic gray cast iron brake disc. In each test, the sample was subjected to four different braking times (3, 6, 9, and 12 minutes) and four applied loads (200, 400, 600 and 800 N). The rotating velocity of the disc was kept constant throughout the friction tests at 750 rpm. After each test, the morphological changes on the surface and subsurface of the material were observed using Scanning Electron Microscopy (SEM). The following characteristics were observed: (i) the surface temperature increased with braking time and after reaching a maximum value, eventually arrived at a steady state, (ii) the friction coefficient increased at the early stages of braking, then decreased with braking time and thereafter reached steady state, and (iii) the wear volume increased linearly when the applied load was below 200 N and/or braking time was below 3 minutes or both, thereafter the volume increased exponentially. Microstructural examinations showed that the wear mechanism transisted with increase in braking times as well as applied loads. This phenomenon also resulted in changes of the wear behaviour.

Keywords: Brake pad, surface temperature, friction coefficient, wear, wear mechanism

Abstrak. Dalam kajian ini, penilaian haus mekanikal ke atas bahan geseran separa logam untuk kegunaan kereta penumpang dikaji dengan menekan sampel kepada piring yang berpusing diperbuat daripada besi tuang kelabu pearlitik. Bagi setiap ujian, sampel dikenakan empat jangka masa pembrekan (3, 6, 9, dan 12 minit) dan empat beban kenaan (200, 400, 600 dan 800 N) yang berlainan. Kelajuan putaran piring brek dikekalkan malar sepanjang pengujian geseran pada 750 psm. Selepas setiap ujian, perubahan morfologi permukaan dan subpermukaan diperhatikan dengan menggunakan mikroskop elektron imbasan (MEI). Hasil kajian menunjukkan ciri-ciri berikut: (i) suhu permukaan meningkat dengan masa pembrekan dan selepas mencapai nilai maksimum, akhirnya sampai kepada keadaan stabil, (ii) pekali geseran telah meningkat pada permulaan pembrekan, kemudian menurun dengan masa pembrekan, dan seterusnya sampai kepada keadaan stabil, dan (iii) isipadu haus meningkat secara lelurus apabila beban kenaan di bawah 200 N dan /atau masa pembrekan di bawah 3 minit dan kedua-duanya seterusnya meningkat secara eksponen. Pemeriksaan mikrostruktur menunjukkan mekanisme haus beralih dengan peningkatan jangka masa pembrekan dan beban kenaan. Fenomena ini juga menyebabkan perubahan kepada sifat haus.

Kata kunci: Pad brek, suhu permukaan, pekali geseran, haus, mekanisme haus

[1] AMREC, Advanced Research Centre, SIRIM Berhad, 34, Jalan Hi-Tech 2/3 Kulim Hi-Tech Park, 09000 Kulim, Kedah, Malaysia

* Corresponding author: Tel: 604 4017166, Fax: 604 4033225, Email: talibria@sirim.my

[2 & 3] Department of Mechanical and Materials Engineering, Faculty of Engineering, Universiti Kebangsaan Malaysia, 43600 UKM Bangi, Malaysia

1.0 INTRODUCTION

Automotive friction materials are complex composite materials. Earlier researches showed that the friction coefficient and wear characteristics of friction materials depend on a number of different factors such as operating variables, material characteristics, surface geometry, type, design and environment [1, 2]. Consequently, there is no wear model available that can predict wear a priori from material properties and contact information [3]. Therefore, in the development of automotive friction materials, most of the formulations are achieved through a trial and error process.

Generally, surface temperature increases with increase in operating variable parameters due to the increase in kinetic energy absorbed by the brake pad during braking. This, in turn, causes changes in the physical and chemical properties [4] as well as thermomechanical behaviour [5]. The polymer material will degrade as the temperature is increased beyond 230°C. Above the degradation temperature, the bond between metal fiber and resin is weakened by thermal metal grains or by more serious thermal expansion of the resin [6]. High temperatures also decrease the yield strength of the materials and leads to changes in the wear mechanism and the real contact configuration [7]. As the surface temperature increases, the adhesion of the transfer layer becomes weak resulting in the flaking of the transfer layers and thus an increase in the wear rate [8].

The friction coefficient is highest at the beginning of braking and slowly decreases with time. The decrease in friction coefficient is probably due to the decomposition of the organic compounds in the braking materials. However, friction coefficient may increase later due to the formation of local carbonisation on the wear surface [9]. The friction coefficient and wear rate become stable when stable transfer films are formed on the composite [10]. Previous researches concluded that the wear mechanisms experienced by the brake lining materials were of types adhesion, abrasion, fatigue, delamination and thermal. Other researchers such as Zhigao and Xiaofei [6], and Talib *et al.* [11] reported that pyrolysis is the controlling mechanism at high temperatures.

In this study, the changes of the physical and mechanical characteristics of an automotive semi-metallic friction material were monitored for the various applied loads and braking times. A semi-metallic material (brake pad) used was steel wools and porous iron powder as the main constituent (65% by weight, where 10 - 25% are steel fibres) and bound together with heat resistant phenolic resins (10%) and other binder or filler materials. The semi-metallic brake pad can be used at higher temperature with stable friction coefficient, low wear, less squeal, and higher energy absorption. The microstructural changes on the surface and subsurface of the wear surfaces were observed using SEM. Based on this observation, the wear behaviour and mechanism which operated during braking were postulated. An attempt was also made to correlate the wear behaviour with the microstructural changes during braking.

2.0 MATERIALS AND METHODS

In this study, a semi-metallic friction material (brake pad) commercially available for passenger car was used. The samples were marked as A, B, C, and D corresponding to the different loads applied. Each sample was then marked with subscripts 1, 2, 3, and 4 for different braking times. Details of the friction material composition are shown in Tables 1 and 2. The organic and inorganic material content in the sample was analyzed using thermogravimetry analysis (TGA) and the metallic composition in the sample was analyzed using Energy Dispersive X-Ray analysis (EDAX). All samples were subjected to friction tests by using a Schenck friction test machine. Figure 1 shows a schematic diagram of the friction test set-up. Test samples were cut from the brake pad backing plate with dimensions of 20 ± 1 mm (length) × 30 ± 1 mm (width) × 15 ± 1 mm (thickness). The samples were glued to the backing plate using ATE glue and placed in the oven at 150°C for at least one hour (Manufacturer's specification, ATE German). This backing plate was then attached to the brake callipers on both sides of the brake disc.

Table 1 Sample composition

Materials	Weight percentage (%)
Organic material	14.22
Inorganic material	85.78

Table 2 Metallic composition (inorganic material) of the sample

Element	Weight %
Mg	1.38
Al	2.38
Si	4.96
S	5.88
K	0.61
Ca	0.87
Ti	5.37
Fe	78.52
Total	100.00

Test samples were subjected to four different applied loads (200, 400, 600 and 800 N) and four different braking times (3, 6, 9, and 12 minutes). The rotating velocity of the brake disc was fixed for all the test conditions at 750 rpm. Test results obtained from the friction test were surface temperature (θ, °C), friction coefficient (μ), and wear volume (W, mm^3). The surface temperature was measured by the thermocouple embedded in the brake disc 1 mm from the surface of the friction

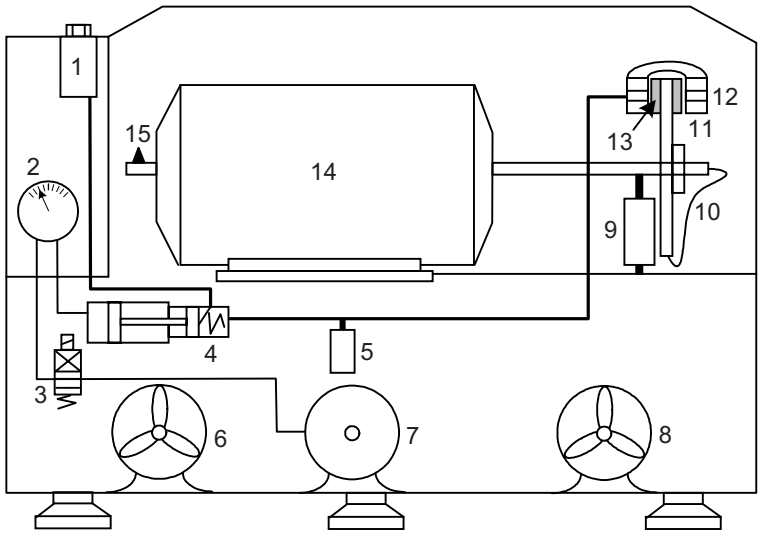

Figure 1 Schematic of brake lining test machine: 1 – brake fluid reservoir, 2 – pressure gauge, 3 – solenoid valve, 4 – air-hydraulic cylinder, 5 – pressure pick-up, 6 – air blower-in, 7 – air tank, 8 – air blower-our, 9 – load cell, 10 – thermocouple, 11 – brake disc, 12 – brake caliper, 13 – friction material, 14 – 75 kW AC motor, 15 – speed sensor

material and was located in the middle of the contact area. After each test, the samples were then subjected to microstructural examination using scanning electron microscopy model PHILIP SL 300. Samples for surface examination were cut from the backing plate, cleaned with compressed air and then coated with gold. Samples for subsurface examination were further cut parallel and perpendicular to the sliding surface using a fine cutter. These were mounted and polished to 1 μm surface finish.

3.0 RESULTS AND DISCUSSION

3.1 Surface Temperature

A braking system converts kinetic energy to heat energy when brake is applied. Kinetic energy absorbed by the brake pad during braking causes the surface temperature to increase. Heat absorbed by the brake pads will be released to the atmosphere through conduction, convection and radiation [12]. It was observed that the surface temperature increases with braking time and after reaching a maximum value, eventually arrived at a thermal steady state (Figure 2). The temperature increment was thought to be purely due to the heat generated by the friction between the sample and rotor. The surface temperature stabilised when the rate of heat generated during braking was balanced by the rate of heat loss to the atmosphere.

All test loads showed the same trend. However, the maximum value and the rate of temperature increase are dependent on the amount of applied load. Test results

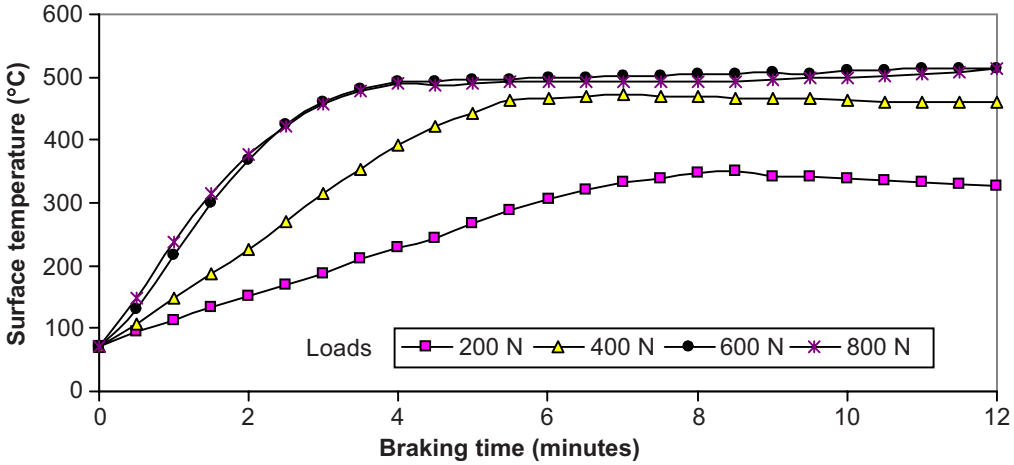

Figure 2 Graph of surface temperature versus braking time

also showed that the temperature increases with the increase in applied load. This phenomenon was thought to be due to the increase in kinetic energy absorbed by the brake pad during braking as a result of higher friction resistance and large contact area. The enlargement of the contact area may be deduced from the microstructural examinations. Figures 3 and 4 show the ploughing marks under applied loads of 200 N and 600 N, respectively. Under the load of 200 N, the ploughing marks were shallow and the distance between the peaks was closer as compared to those that appeared on the sample loaded to 800 N, which were deeper. Under higher load, the peak asperities ploughed deeper into the wear surface, thus increasing friction resistance. Figures 5 - 8 show the increase of contact area with the increase in applied load. This also contributes to the increase of temperature with increasing of applied load.

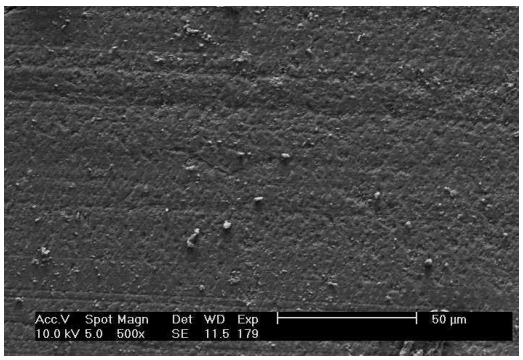

Figure 3 The peak asperities ploughing on the surface of the sample. Load 200 N, time 3 minutes

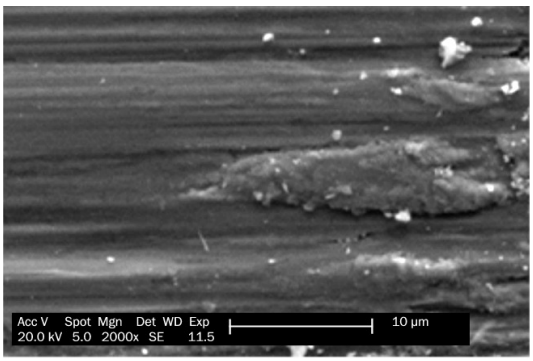

Figure 4 Micrograph shows surface after ploughing under higher applied load of 800 N, time 3 minutes

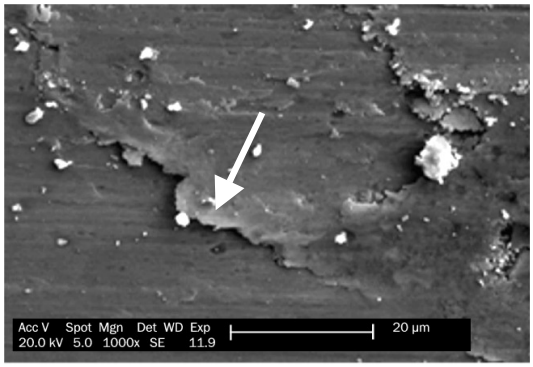

Figure 5 Micrograph shows the wear fragment to be detached from the surface. Load 200 N, time 6 minutes

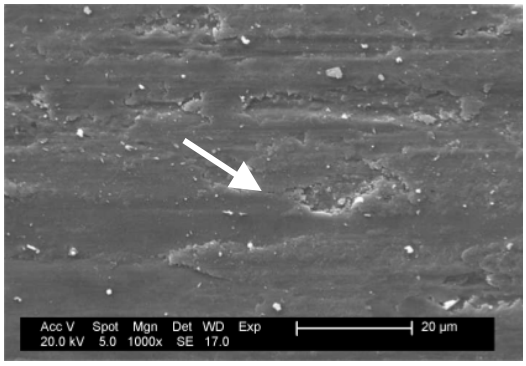

Figure 6 Subsequent brakings result in transfer patches being flattened and sheared on the worn surface. Load 400 N, time 6 minutes

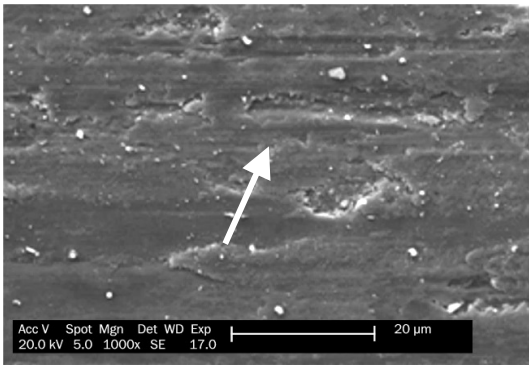

Figure 7 Subsequent braking results in the formation of transfer layers on the worn surface. Load 200 N, time 9 minutes

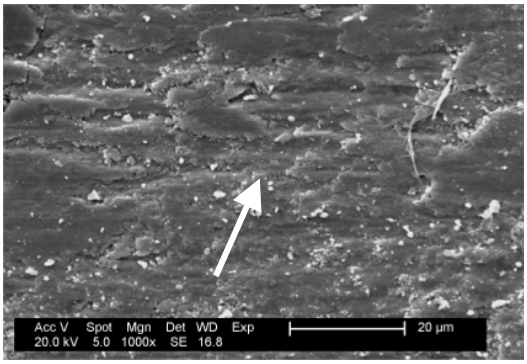

Figure 8 Multilayer transfer layers were formed as the braking time increased. Load 400 N, time 12 minutes

The following features were also observed; (i) The surface temperature stabilised faster with the increase of applied loads and reached maximum value when the applied load is greater than 600 N, and (ii) The rate of temperature rise is highest (137.1 degree/min) when the applied load is greater than 600 N (Figure 2). This was probably due to the design of the thermal conductivity of the friction material, which in this case is maximum under this load. The higher the load applied during braking, the higher in friction resistance, thus the temperature.

3.2 Friction Coefficient

In the braking process, the brake is pressed against a rotating brake disc, resulting in resistance to motion. With increasing applied load, the friction coefficient has reached

faster to a maximum value. It then decreased with braking time and thereafter reached a steady state (Figure 9). The increase of friction coefficient at the beginning of braking was due to the harder asperities being ploughed into the wear surfaces and also due to the enlargement of the contact area. At the early stage of braking, harder asperities were ploughed into the wear surfaces as can be seen from Figures 3 and 4. The ensuing reduction of friction coefficient may be explained by (i) the shearing of the peak asperities and (ii) formation of friction film and (iii) decomposition of the organic compounds. Figure 5 shows the detachment of wear fragment from the wear surface at the early stage of braking. With subsequent braking, the asperities were sheared and blunted during sliding (Figure 6). This process resulted in interlocking between asperities to be reduced and hence, the friction.

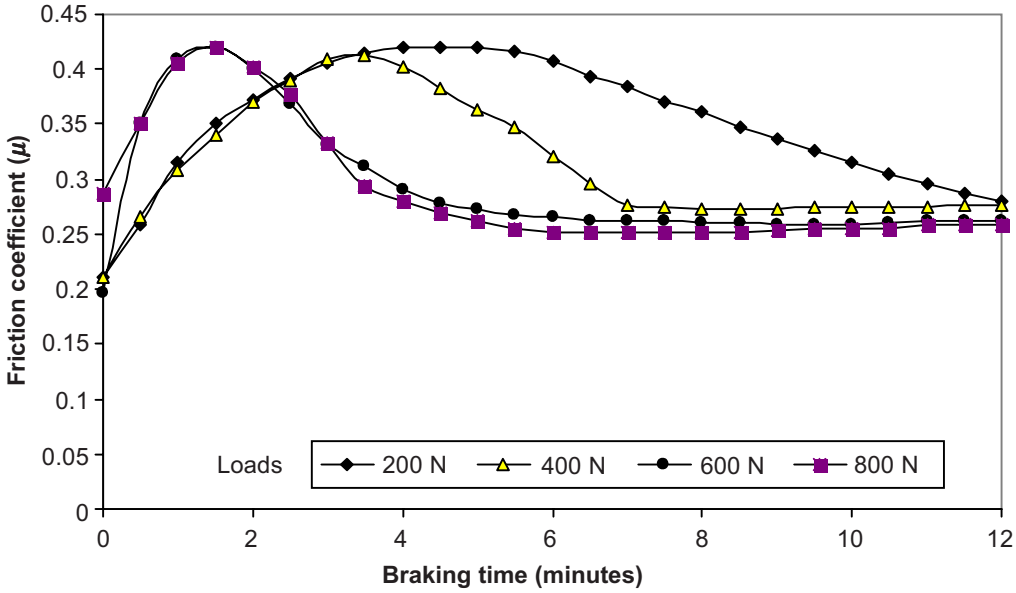

Figure 9 Graph of friction coefficient versus braking time

Figures 7 and 8 show the formation of a transfer layer or friction film on the worn surface. The formation of the transfer layer is the results of wear debris compaction between the brake pad and disc surfaces [13]. As the thermal degradation increased with braking time, the mechanical integrity of the compacted wear debris became progressively weaker. Figure 10 shows the formation of plastic flow due to high temperature. The compacted layers would become very weak as thermal degradation proceeded, perhaps resulting in a situation of a three-body rolling contact, in which friction coefficient will be reduced [14]. In this study, the existence of wear particles in the shapes of spheres, cylinders and plates (Figure 11) are postulated to be a consequence of the above described process.

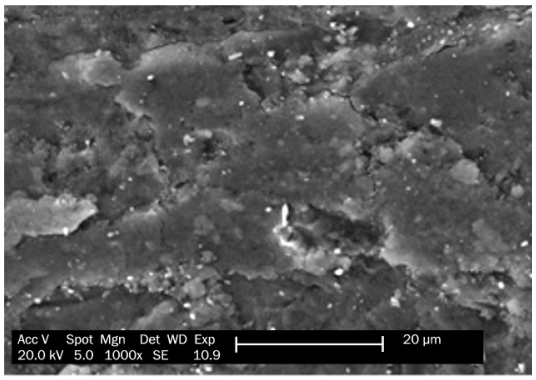

Figure 10 SEM micrograph shows the plastic flow formation on the wear surface. Load 800 N and time 9 minutes

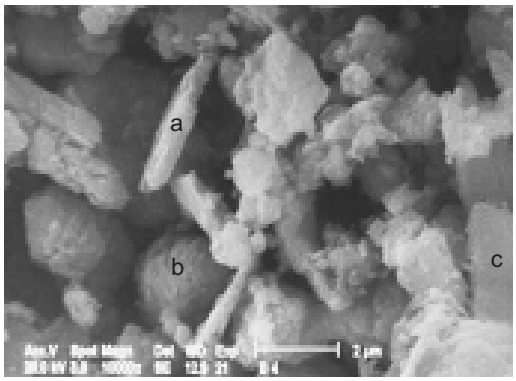

Figure 11 Wear particles in the shape of (a) cylinder, (b) sphere, (c) plate. Load 600 N, time 12 minutes

Test results show the friction coefficient has reached a maximum value when the surface temperature was above the degradation temperature (230°C) depending on the load applied (Table 3). After reaching a maximum value, then the friction coefficient decreased with increasing surface temperature and thereafter became stable as the temperature reached a stable value (Figure 12). This phenomenon was thought to be due to the degradation of the organic compounds in the formulation which increases with temperature. The evaporation of organic material may generate pressure at the surface between the brake friction material and mating surfaces. Begelinger and Gee reported that this might provide aerodynamic gas lubricant, thus dramatically lowering friction [9]. As the friction is reduced, the heat generated during braking would also be reduced. Microstructural examinations (Figures 6, 7, and 8) show a formation of a continuous friction film on the wear surfaces which become stabilized with increase in braking time, resulting in a stable value of friction coefficient as shown in Figure 9.

Table 3 Maximum friction coefficient

Applied load (N)	Maximum friction coefficient	Surface temperature (°C)
200	0.41	266
400	0.41	354
600	0.42	300
800	0.42	315

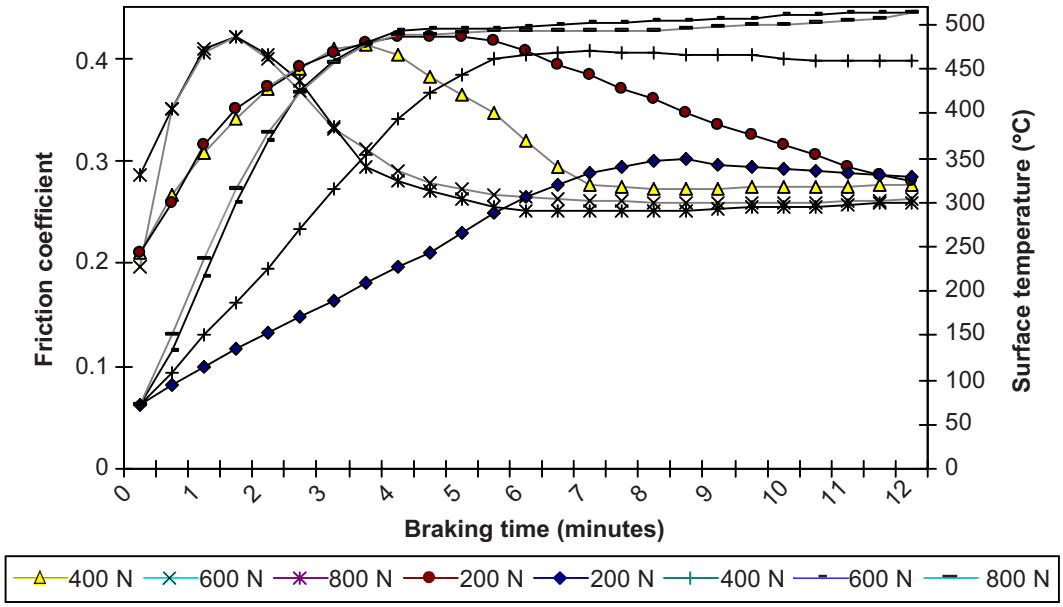

Figure 12 Graph of friction coefficient and surface temperature versus braking time

3.3 Wear Volume

The wear volume increased exponentially when the applied load more than 200 N and/or braking time more than 3 minutes or both. Below this condition, the wear volume increased linearly (Figure 13). This is due to the following phenomena; (i) the decomposition of organic materials, (ii) microstructural changes and (iii) transition of wear mechanism. The degradation of the organic components in the brake pad composition increased with surface temperature and this resulted in the reduction of composition bonding and structure integrity. This process may have increased the rate of surface failure, thus increasing wear rate exponentially, as observed in this work. This finding is similar with the results reported by other researchers such as Zhigao and Xiaofei [6], and Talib *et al.* [11].

Increasing the braking times as well as applied loads resulted in an increase in the surface temperatures (Figure 2). Previous studies have attributed this to several reasons, such as the destruction of surface deformation [5], a decrease in yield strength [7] and the destruction of the friction film [8]. Higher temperatures also caused an extensive plastic flow resulting in the pile-up of deformed material on the worn surface (Figure 10). Subsequently, this material could be sheared off at the edge of the sliding surfaces, resulting in material loss. Figure 11 shows the morphology of the wear particles. This could explain why the wear volume in this study increased exponentially with time.

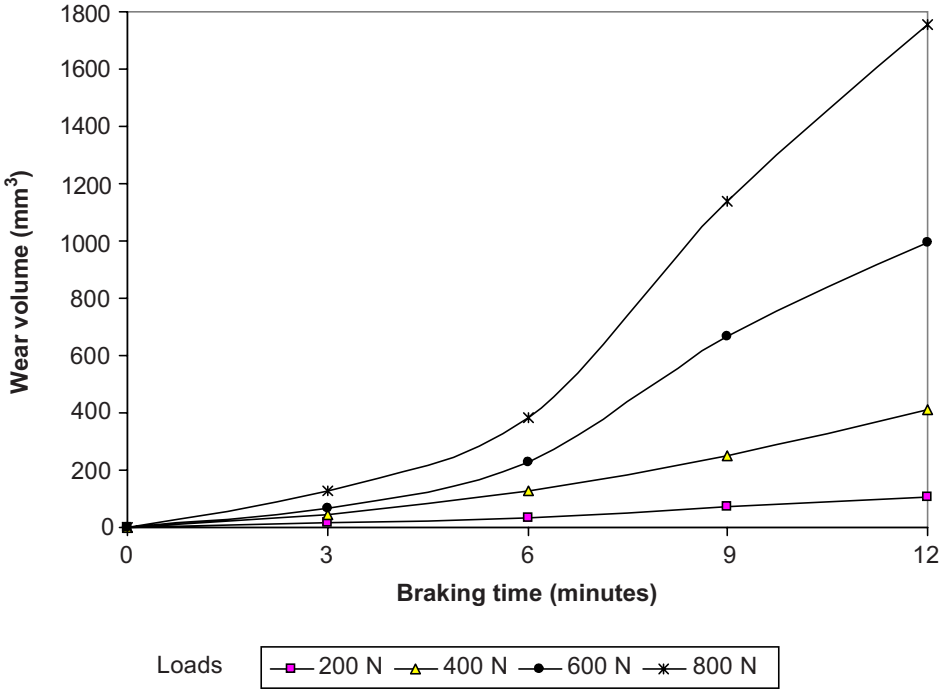

Figure 13 Graph of wear volume versus braking time

In 1970, Rhee introduced an empirical wear equation for predicting wear of asbestos-reinforced polymers when sliding against cast iron and chromium copper drum in the form of $\Delta W = KP^a V^b t^c$ [15], where ΔW is the weight loss, K is the wear factor, P is the load, V is the velocity, t is the time of sliding, and a, b, and c are constants. He found that the wear could be described satisfactorily by the wear equation introduced. The parameters a, b and c were determined experimentally by varying only one variable at a time and keeping the other two variables constant. The value of a is the slope of line log W vs. log P and the value of c is the slope of line log W vs. log t. In this study, the value of b is assumed to be 1 as the effect of speed is not investigated due to the limitation of the test machine. The wear data were plotted against applied load and braking time as shown in Figures 14 and 15 respectively.

In this work, it was found that there are two sets of the parameter a and c depending on the applied load and braking time. The test results for different set of combination of applied load 200 N and/or braking time 3 minutes is summarised in Table 4. Under this condition, the wear factor was found to vary from 3.296×10^{-7} to 94.804×10^{-7}. Thus, the proposed formula cannot be applied under this condition. When the value of parameters a and c change to $a = c = 1$, the wear factor becomes constant, varies from 1.1671×10^{-4} to 2.1079×10^{-4} (Table 5). This shows that the wear increase linearly when the applied load is below 200 N and/or braking time or

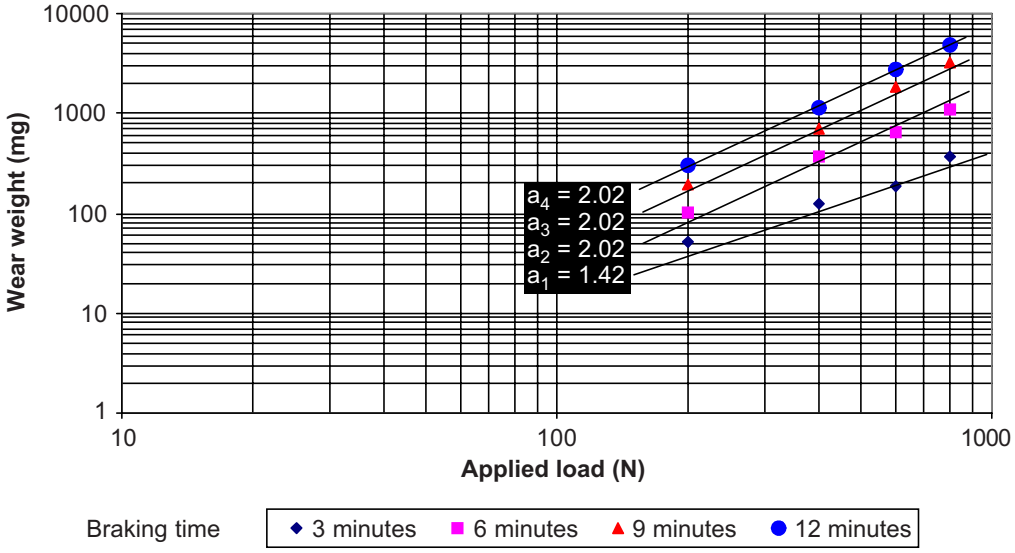

Figure 14 Dependence of wear on applied load

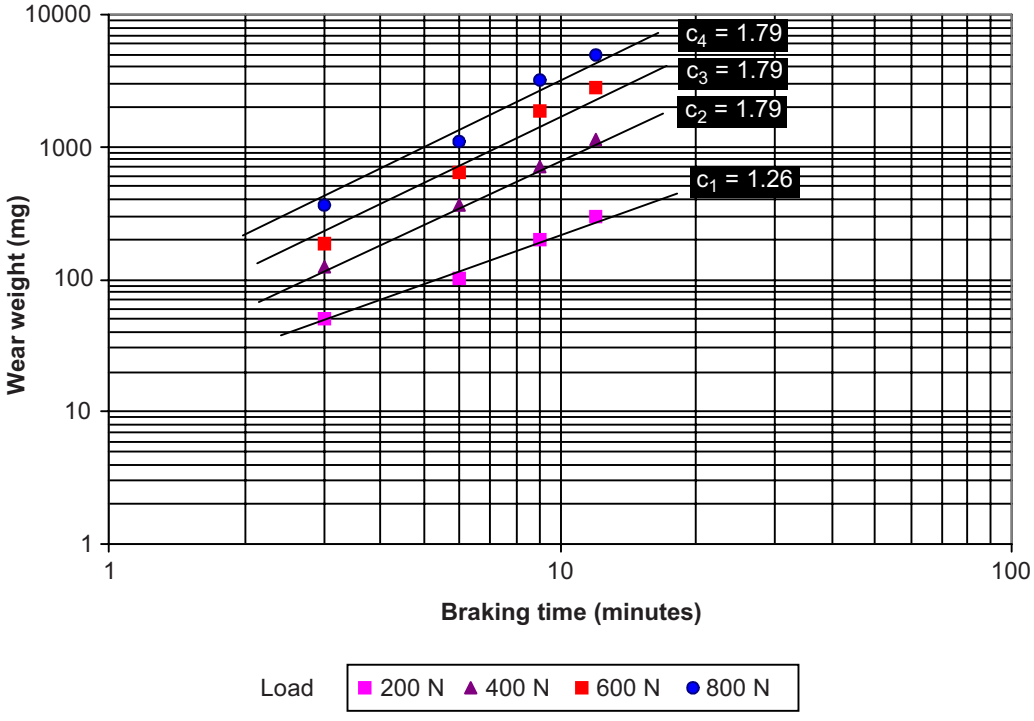

Figure 15 Dependence of wear on braking time

Table 4 Wear data with a combination of load 200 N and/or braking time of 3 minutes or both

Load (N)	Speed (rpm)	Time (min)	Wear (gm)	*a*	*b*	*c*	Wear factor $K \times 10^{-6}$
200	750	6	105.08	1.42	1	1.79	3.296
200	750	9	204.60	1.42	1	1.79	3.851
200	750	12	310.09	1.42	1	1.79	4.062
200	750	3	52.52	1.42	1	1.26	94.804
400	750	3	128.30	2.02	1	1.26	48.299
600	750	3	193.25	2.02	1	1.26	40.095
800	750	3	379.43	2.02	1	1.26	53.380
						Average	35.51

Table 5 Wear data with a combination of load 200 N and/or braking time of 3 minutes or both when parameter $a = b = c = 1$

Load (N)	Speed (rpm)	Time (min)	Wear (gm)	*a*	*b*	*c*	Wear factor $K \times 10^{-4}$
200	750	6	105.08	1	1	1	1.1676
200	750	9	204.60	1	1	1	1.5156
200	750	12	310.09	1	1	1	1.7227
200	750	3	52.52	1	1	1	1.1671
400	750	3	128.30	1	1	1	1.4256
600	750	3	193.25	1	1	1	1.4315
800	750	3	379.43	1	1	1	2.1079
						Average	1.5054

below 3 minutes and the equation reduces to linear relationship as proposed by Holm [16]:

$$\Delta W = KPVt$$

where ΔW is in g, F is in N, V is in r.p.m. and t is in minute.

The values of a and c when the applied load with a combination of load of 400 N and above and/or braking time of 6 minutes and above or both are shown in Table 6. The parameters are found to be constant: $a = 2.02$, and $c = 1.79$. The wear factor was found constant in all cases, varies from $8.2552 \times$ to 12.363×10^{-8}. Thus, the wear under this condition can be described by the equation:

$$\Delta W = KP^{2.02}Vt^{1.79}$$

where ΔW is in g, F is in N, V is in r.p.m. and t is in minute.

Based on the above observations, two general correlations existed for this material; a linear relationship as well as an exponential one. The linear relationship was found

Table 6 Wear data with a combination load of 400 N and above or braking time of 6 minutes and above or both

Load (N)	Speed (rpm)	Time (min)	Wear (gm)	*a*	*b*	*c*	Wear factor $K \times 10^{-8}$
400	750	6	375.36	2.02	1	1.79	11.229
400	750	9	724.3	2.02	1	1.79	10.486
400	750	12	1190.3	2.02	1	1.79	10.298
600	750	6	661.85	2.02	1	1.79	8.729
600	750	9	1937	2.02	1	1.79	12.363
600	750	12	2886.5	2.02	1	1.79	11.008
800	750	6	1119.2	2.02	1	1.79	8.2559
800	750	9	3317.3	2.02	1	1.79	11.841
800	750	12	5100.9	2.02	1	1.79	10.880
						Average	10.566

to be operative when the applied load was below 200 N and braking time less than 3 minutes or both. Whereas the exponential one was found to be operating above when the applied load was more than 200 N and/or braking time was more than 3 minutes or both.

3.4 Wear Mechanism

In the present study, microstructural changes on the worn surface of the brake pads manifested the following major wear mechanisms; (i) abrasive (ii) adhesive (iii) fatigue (iv) delamination and (v) thermal. The overall wear mechanism and wear transition from one mechanism to another were influenced by the braking times and applied loads.

3.4.1 Abrasive Wear

At the onset of braking, the harder asperities in the structures were ploughed into the wear surfaces under all applied load conditions (Figure 3). This process was a manifestation of abrasion mechanisms. It was also noticed that the surface became rougher as the applied load was increased (Figure 4). This phenomenon was a result of deeper penetration of the peak asperities on the brake pad surfaces as the load was increased. On subsequent braking, the asperities were sheared and became blunt making the wear surface smoother (Figure 6). After 9 minutes, however, no more abrasive wear was observed. Abrasive wear was found only at the early stage of braking. Thus, this mechanism was not a major contributor to the overall wear phenomena but played a major role on the friction resistance at the early stage of braking, as shown in Figure 9.

3.4.2 Adhesive Wear

Microstructural investigation also showed the formation and shearing of transfer patches on the wear surface (Figures 5 and 6). These were manifestations of the adhesion wear mechanisms. On the second braking (6 minutes), the asperities were sheared, causing the wear surfaces to be covered with transfer layers, which had been compacted, smeared, sheared and flattened (Figure 7). With subsequent braking, the wear surfaces were covered with multiple transfer layers (Figure 8). When the load was increased up to 600 N, plastic flow of the transfer layer was observed after a braking time of 12 minutes (Figure 10). Under this test condition, the bulk temperature recorded was 514°C but the flash temperature during contact could be as high as between 1000°C to 1125°C [17]. As a result of these high temperatures, the transfer layers melted and plastic flow occurred on the worn surface. Microstructural examinations revealed that the adhesion mechanism is a continuous process and the degree of adhesion increased with increasing of braking times and applied loads. This correspond well with the wear volume as shown in Figure 13. These microstructural changes also correspond with the friction coefficient characteristics (Figure 9) where the friction coefficient increased with the severity of the adhesion mechanism.

3.4.3 Fatigue Wear

The surface of friction materials is still rough even after braking as shown in Figure 16. The non-uniform rotor thickness is typically called Disc Thickness Variation (DTV) may cause the peak asperities to be subjected to cyclic contact (Figure 17).

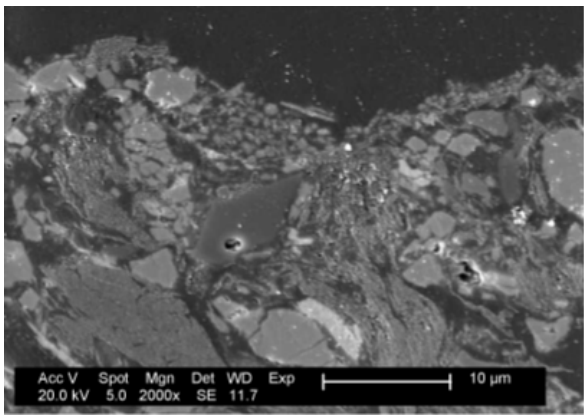

Figure 16 SEM of surface profile after braking with applied load of 200 N and braking time of 3 minutes. Distance between peaks 34 μm dan distance peak and valley 8 μm

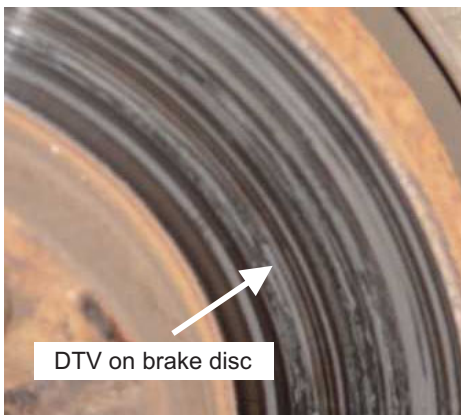

Figure 17 Photograph of disc thickness variation on contact area

DTV can be created in a number of ways; (i) new rotor flatness, (ii) rotor/pad corrosion, (iii) rotor 'hot spots', and (iv) thermal deformation of the rotor [18]. After repeated contact, fatigue microcracks will be generated at the point of maximum stress and minimum local strength [19]. These microcracks can propagate and grow due to repeated normal and tangent shear during sliding and fatigue wear was observed in the form of striations, pits, spalls and microcracks.

The fatigue mechanism was found to be only in the operation under the applied load of 200 N. Fatigue mechanism starts with the formation of striations on the surface due to the cyclic-plastic deformation. In this work, striations were first observed during a braking time of 6 minutes at 200 N load (Figure 18). The distance between striations increases with the increasing of braking time (Figure 19). With subsequent braking, fatigue microcracks nucleated at the edges of the transfer layers and at

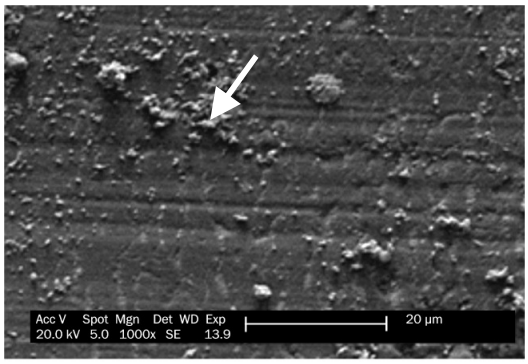

Figure 18 Early stage of striation formation. Load 200 N, time 6 minutes

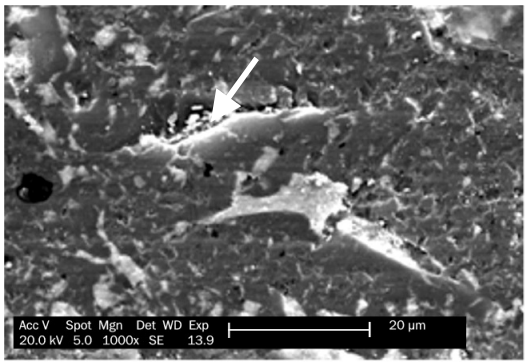

Figure 19 Micrograph shows the appearance of striations with generation of fatigue microcrack. Load 200 N, time 6 minutes

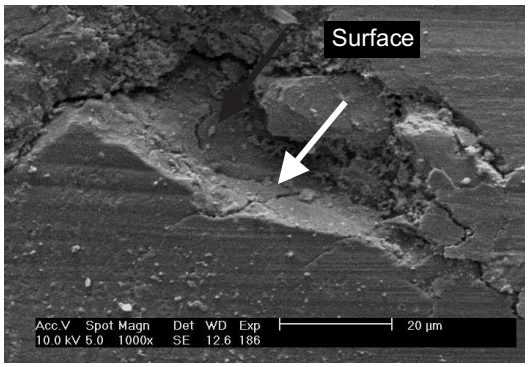

Figure 20 Fatigue microcrack nucleated places where pits and spalls were found. Load 200 N, time 9 minutes

places where pits and spalls were found (Figure 20). As no fatigue wear was observed when the applied load was more than 200 N, it is suggested that this wear mechanism was not a major contributor to friction coefficient of the brake pad during braking.

3.4.4 Delamination Wear

In the early stage of delamination process, plastic deformation is generated due to repeated contact during braking process (Figure 21). As the braking proceeded, dislocations were generated due to the accumulation of plastic deformation in the subsurface. The generation of delamination wear is due to dislocation pile-up as the movements of the dislocations are blocked by the presence of inclusions and hard particles [20]. Figure 22 shows microcrack generated surround hard particle in the

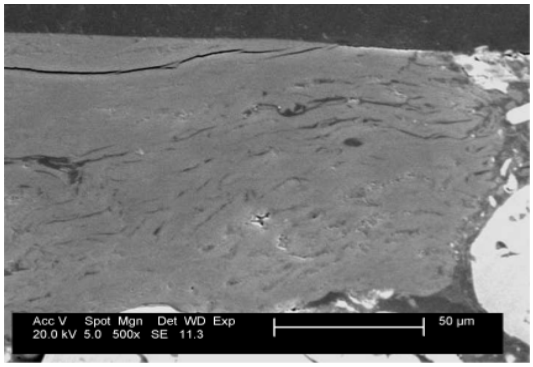

Figure 21 Micrograph shows a number of deformation bands parallel to the wear surface under applied load of 200 N and braking time of 9 minutes

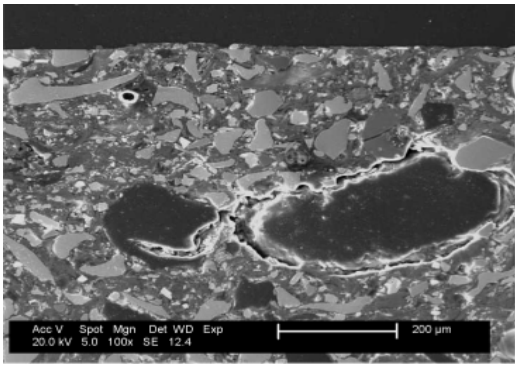

Figure 22 Micrograph shows the generation of subsurface microcrack due to coalescence of second phase particles. Applied load 200 N and braking time 15 minutes

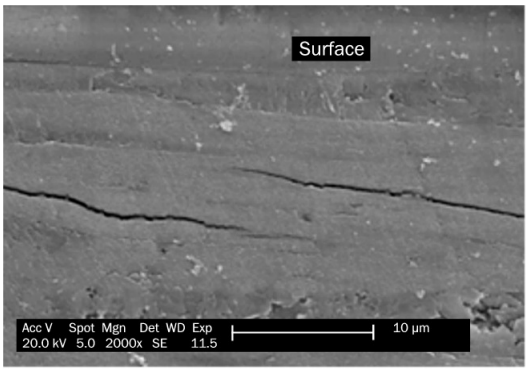

Figure 23 The propagation of a microcrack beneath the wear surface. Load 400 N, and time 3 minutes

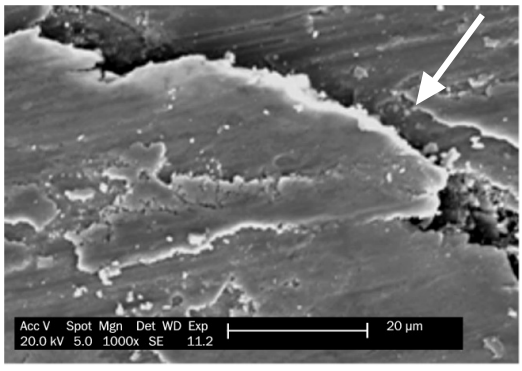

Figure 24 Micrograph showing wear fragment to be delaminated from the wear surface. Load 200 N, and time 6 minutes

composition of brake pad materials. As a result of dislocation pile-up, microcracks were generated parallel to the wear surfaces as shown in Figure 23. The delamination wear mechanism was first seen during the third braking (12 minutes) under the applied load of 200 N. When the applied load was increased to 400 N and above, the delamination mechanism was generated earlier at a braking time of 9 minutes. As the braking proceeded, wear fragments were delaminated from the worn surface (Figure 24). The delamination mechanism was significant when the applied load was more than 400 N and braking time was more than 9 minutes. Under these conditions, the wear volume was very high (Figure 13) whereby more materials were removed by the delaminated mechanism as compared to the other mechanisms.

3.4.5 Thermoinstability

In the present study, thermal granules were observed. These were generated due to thermoinstability as a result of high temperature. Figure 25 shows that thermal granules were located above the wear surfaces and thus became the contact area as the sliding progressed. As the applied loads or braking times were increased, the temperature rose at the contact area that introduced thermal stresses, which could superimpose onto the mechanical stresses [21]. This condition resulted in very high contact stresses, which caused the generation of thermomicrocracks.

Thermal granules were first seen after braking time of 9 minutes when the applied load was 200 N. As the load was increased to 400 N and 600 N, thermal granules were generated earlier at braking times of 6 and 3 minutes respectively. With time, the thermal granules were compacted and sheared forming thermal patches as shown in Figure 26. Upon experiencing very high total contact stresses, these became thermomicrocracks. Thermomicrocracks were first seen after braking for 12 minutes when the applied load was 200 N. Thermomicrocracks were generated earlier upon increasing the applied load. With subsequent braking, the microcracks grew,

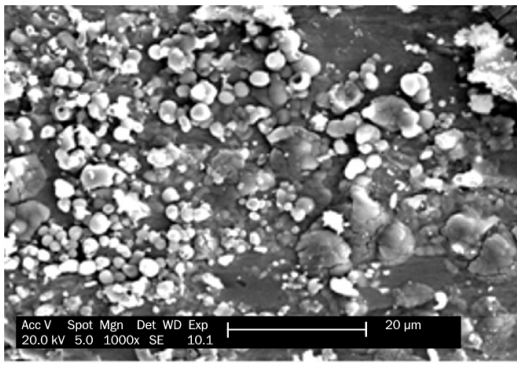

Figure 25 Formation of thermal granules. Load 800 N, and time 3 minutes

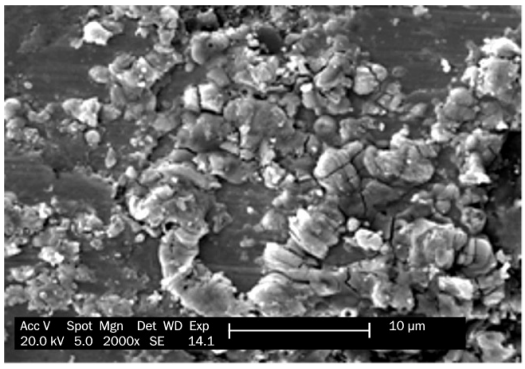

Figure 26 Generation of thermal patches. Load 800 N, and time 6 minutes

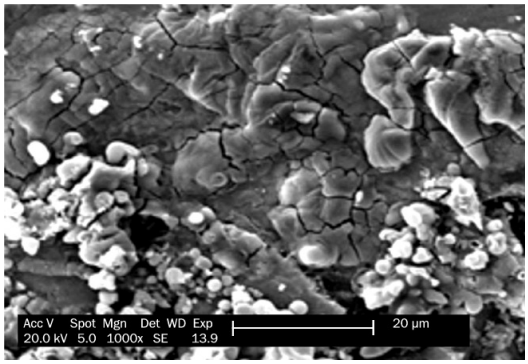

Figure 27 Formation of multiple thermal microcracks. Load 600 N, time 9 minutes

propagated and finally interconnect with each other to form multiple microcracks (Figure 27). As previously shown in Figure 13, the wear volume increased progressively with applied load and this corresponded with the generation of the thermomicrocracks.

The microstructural examinations showed that the wear mechanism transisted from one combination to another as the braking times and applied loads were increased. For example, when the brake was operated under a load of 200 N, the wear mechanism transisted from a complex mixture of adhesion and abrasion to a complex mixture of adhesion, fatigue, delamination and thermal wear. When the applied load was increased to 400 N, the wear mechanism transisted from a complex mixture of adhesion and abrasion to a complex mixture of adhesion, delamination and thermal wear. Subsequently, when the load was increased to 600 N and higher, the wear mechanism transisted from a complex mixture of adhesion, abrasion and thermal to a complex mixture of adhesion, thermal and delamination wear. The transition period is found to be dependent on load used.

4.0 CONCLUSIONS

In the present study, the following phenomenon were found to occur during the braking process when a semi-metallic automotive friction material was pressed against a rotating gray cast iron brake disc;

(i) Friction coefficient was highest on the onset of braking due to ploughing of harder asperities and enlargement of the contact area. Thereafter, friction slowly decreased with braking time due to shearing of the peak asperities and formation of a friction film.

(ii) Wear volume increased linearly when the applied load was below 200 N and/or braking time was below 3 minutes or both, thereafter the volume increased exponentially. This was due to the transition of wear mechanism, in correspondence with the microstructural changes and the decomposition of organic materials.

(iii) It was observed that the wear mechanism during braking is rather complex and no single mechanism could explain the phenomenon. The major wear phenomena observed during braking processes were; (i) abrasive (ii) adhesive (iii) fatigue (iv) delamination and (v) thermal wear. The wear mechanism in the operation during braking was dependent on the applied loads and braking times.

ACKNOWLEDGEMENTS

The cooperation and assistance of the Mechanical and Automotive Engineering Testing Unit and Metal Performance Centre, SIRIM Berhad staff are greatly appreciated.

REFERENCES

[1] Filip, P., L. Kovarik, and M. A. Wright. 1995. Automotive Brake Lining Characterization. Proceeding of the 8th International Pacific Conference on Automobile Engineering. Yokohama, Japan.

[2] Talib, R. J., K. Ramlan, and C. H. Azhari. 2001. Wear of Friction Materials for Passenger Cars. *Journal Solid State Science & Technology*. 10(1, 2): 292-298.

[3] Hsu, S. M., M. C. Shen, and A. W. Ruff. 1997. Wear Prediction for Metals. *Tribology International*. 30: 377-383.

[4] Sasaki, Y. 1995. Development Philosophy of Friction Materials for Automobile Disc Brakes. The 8th International Pacific Conference on Automobile Engineering. 4-9 November. Yokohama. Society of Automobile Engineers of Japan. 407-412.

[5] Kennedy, Jr. F. E. 1980. Thermomechanical Phenomena in High Speed Rubbing. *Wear*. 59: 149-163.

[6] Zhigao, X. and L. Xiaofei. 1991. A Research for the Friction and Wear Properties of a Metal-fiber-reinforced Composite Material. In Boqun Wu (Ed.). *Mechanical Properties Materials Design 5*. Amsterdam: Elsevier Science Publisher. 611-615.

[7] So, H. 1996. Characteristics of Wear Results Tested by Pin-on Disc at Moderate to High Speeds. *Tribology International*. 29(5): 415-423.

[8] Jacko, M. G., P. H. S. Tsang, and S. K. Rhee. 1989. Wear Debris Compaction and Friction Film Formation of Polymer Composites. In K. C. Ludema, (Ed.). *Wear of Materials*. New York: American Society of Mechanical Engineers. 469-481.

[9] Begelinger, A. and A. W. J. Gee. 1973. *A New Method for Testing Brake Lining Material*. ASTM Special Technical Publication 567. Philadelphia: American Standard for Testing and Materials. 316-334.

[10] Siwei, Z. 1991. Studies in Non-asbestos Friction Materials: A Brief Review. In Boqun Wu (Ed.). *Mechanical Properties Materials Design*. Amsterdam: Elsevier Science Publisher. 403-411.

[11] Talib, R. J. 1995. Investigation on the Wear Mechanism of Brake Pads. MSc. Thesis. National University of Malaysia, Malaysia.

[12] Limpert, R. 1992. *Brake Design and Safety*. Warrendale, USA: Society of Automotive Engineers.

[13] Talib, R. J., A. Muchtar, and C. H. Azhari. 2002. Pad Brek Kenderaan Persendirian: Kajian ke atas Mikrostruktur Lapisan Pindah. *Jurnal Teknologi*. 36(A): 1-12.

[14] Rhee, S. K., M. G. Jacko, and P. H. S. Tsang. 1991. The Role of Friction Film in Friction, Wear and Noise of Automotive Brakes. *Wear*. 146: 89-97.
[15] Rhee, S. K. 1970. Wear Equation for Polymers Sliding Against Metal Surfaces. *Wear*. 16: 431-445.
[16] Holm, R. 1946. *Electric Contact*. Stockholm: Almquist and Wikksells.
[17] Anderson, A. E. 1980. Wear of Brake Material. In M. Peterson and W. O Winer (Eds.). *Wear Control Handbook*. New York: ASME. 843-858.
[18] Greening, C. W. Jr. 2006. Basics of Brake Disc Thickness Variation and Judder. Fourth Malaysian Friction Materials Colloquium 2006. Langkawi, Malaysia.
[19] ASM. 1992. *ASM Metal Handbook 11*. Failure and Analysis Prevention. USA: American Society for Metals.
[20] Suh, N. P. 1973. The Delamination Theory of Wear. *Wear*. 25: 111-124.
[21] Ting, B. Y. 1988. A Thermomechanical Wear Theory. Dissertation Ph.D. Georgia Institute of Technology, Atlanta.